Chapter 23

Secondary Iron-Sulfate Minerals as Sources of Sulfate and Acidity

Geochemical Evolution of Acidic Ground Water at a Reclaimed Surface Coal Mine in Pennsylvania

C. A. Cravotta III

U.S. Geological Survey, 840 Market Street, Lemoyne, PA 17043

Despite negligible concentrations of dissolved oxygen (O_2) in ground water, concentrations of sulfate (SO_4^{2-}) and acidity increase with depth along paths of ground-water flow from the water table in mine spoil through underlying bedrock at a reclaimed surface coal mine in the bituminous field of western Pennsylvania. This trend can result from the oxidation of pyrite (FeS_2) in the unsaturated zone, transport of oxidation products, and additional oxidation in the saturated zone. FeS_2 can be oxidized by O_2 or by ferric ions (Fe^{3+}) in the absence of O_2. In acidic water, Fe^{3+} is more soluble than O_2. Iron-sulfate hydrates, including römerite [$Fe^{II}Fe_2^{III}(SO_4)_4 \cdot 14H_2O$], copiapite [$Fe^{II}Fe_4^{III}(SO_4)_6(OH)_2 \cdot 20H_2O$], and coquimbite [$Fe_2^{III}(SO_4)_3 \cdot 9H_2O$], are associated with FeS_2 in coal from the mine. These soluble salts can form on the surface of oxidizing FeS_2 in unsaturated mine spoil, coal, and overburden, and can dissolve in ground water thereby releasing SO_4^{2-} and Fe^{3+}. Subsequent oxidation of pyritic sulfur by Fe^{3+} and (or) hydrolysis of Fe^{3+} will produce acid under water-saturated conditions, even if O_2 is not present in the system.

Acidic mine drainage (AMD) can result from the accelerated oxidation of iron-disulfide minerals (FeS_2), mainly pyrite, that are exposed to oxygen (O_2) during coal mining (1-6). Accordingly, various schemes have been proposed to reduce the contact between O_2 and FeS_2, including submerging pyritic mine spoil in water (7, 8) or adding organic waste as an O_2-consumptive barrier (9). Because oxidation is rapid, however, secondary iron-sulfate minerals can form during mining and can supply acidity and solutes even in anoxic systems.

During 1986-89, the U.S. Geological Survey, in cooperation with the Pennsylvania Department of Environmental Resources, conducted an investigation at a reclaimed surface coal mine in western Pennsylvania to evaluate effects on ground-water quality from the addition of municipal sewage sludge to mine topsoil. The primary goal of the sludge application was to promote revegetation; a secondary goal was to create an O_2-consumptive barrier. If O_2 in recharge water could be
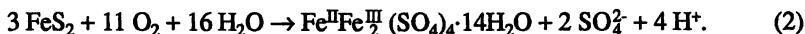
depleted by decay of the sludge, FeS_2 oxidation in underlying mine spoil could be abated. Although concentrations of dissolved O_2 (DO) were negligible [less than 0.034 mmol/kg (millimoles per kilogram)] in ground water from sludge-treated and untreated mine spoil, concentrations of sulfate (SO_4^{2-}) and acidity increased with depth below the water table. This trend can result from the oxidation of FeS_2 in the unsaturated zone, transport of oxidation products, and additional oxidation in the saturated zone. This paper reviews geochemical reactions involving FeS_2 and iron-sulfate hydrate minerals that are likely to produce acidic ground water in O_2-limited systems, and presents results of geochemical mass-balance calculations. The purpose is to evaluate whether availability of O_2 is a limiting factor in acidity generation along ground-water flow paths through mine spoil and bedrock. This evaluation incorporates revised sulfur data used for previous modeling at the site (10), which allows for more narrow constraint of the mass-balance models.

Secondary Iron-Sulfate Minerals as Sources of Acidity

The complete oxidation of pyrite in weakly acidic to neutral systems (pH 4-7) (3-6) can be written as

$$FeS_2 + 3.75\,O_2 + 3.5\,H_2O \rightarrow Fe(OH)_3 + 2\,SO_4^{2-} + 4\,H^+. \qquad (1)$$

In acidic weathering environments, however, iron-sulfate hydrate minerals can form instead of ferrihydrite [$Fe(OH)_3$] (5, 6, 11-16). For example, römerite can form by the oxidation of pyrite,

$$3\,FeS_2 + 11\,O_2 + 16\,H_2O \rightarrow Fe^{II}Fe_2^{III}(SO_4)_4 \cdot 14H_2O + 2\,SO_4^{2-} + 4\,H^+. \qquad (2)$$

For each mole of FeS_2 oxidized, 1/3 of the quantities of dissolved SO_4^{2-} and H^+ produced in reaction 1 are produced in reaction 2; the remaining 2/3 of the "acidity" is stored as unhydrolized, partly oxidized iron (Fe) in the solid phase. In addition to römerite, copiapite [$Fe^{II}Fe_4^{III}(SO_4)_6(OH)_2 \cdot 20H_2O$] and coquimbite [$Fe_2(SO_4)_3 \cdot 9H_2O$] are associated with FeS_2 in high-S coal [S greater than 2 wt % (weight percent)] from the study area. These and other iron-sulfate hydrate minerals can form as oxidation products on the surface of iron-sulfide minerals in stockpiled coal, reclaimed mine spoil, and dewatered, unmined rock. They also can precipitate from oxidizing and evaporating Fe-and-SO_4-rich solutions at AMD discharge zones or at the capillary fringe in the unsaturated zone (6, 14-16).

Because iron-sulfate hydrate minerals are highly soluble (6), they provide an instantaneous source of acidic water upon dissolution and hydrolysis, as shown by the dissolution of römerite

$$Fe^{II}Fe_2^{III}(SO_4)_4 \cdot 14H_2O \rightarrow 2\,Fe(OH)_3 + Fe^{2+} + 4\,SO_4^{2-} + 6\,H^+ + 8\,H_2O. \qquad (3)$$
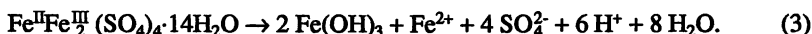
Subsequent oxidation of the ferrous ion (Fe^{2+}) and hydrolysis of the ferric ion (Fe^{3+}) at pH greater than 2 will produce additional acidity according to the overall reaction

$$Fe^{2+} + 0.25\,O_2 + 2.5\,H_2O \rightarrow Fe(OH)_3 + 2\,H^+. \qquad (4)$$

Hence, iron-sulfate hydrate minerals are important as both sinks and sources of AMD by storing acid, Fe, and SO_4^{2-} in a solid phase during dry periods and by releasing the solutes when dissolved during wet periods (10, 14, 17).

Storage of Fe^{3+} in sulfate minerals and its subsequent release into ground water also are an important aspect of oxidation below the water table, because coupled Fe^{3+} reduction and FeS_2 oxidation can occur in anoxic systems (2, 18-22) as follows:

$$FeS_2 + 14\ Fe^{3+} + 8\ H_2O \rightarrow 15\ Fe^{2+} + 2\ SO_4^{2-} + 16\ H^+. \qquad (5)$$
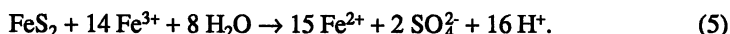
Thus, as the water table rises or as recharge water percolates through the unsaturated zone of mine spoil or unmined rock, dissolution of iron-sulfate minerals and subsequent ferric oxidation of FeS_2 can result. For example, the following overall reaction of pyrite and römerite generates acid in the absence of O_2:

$$FeS_2 + 7\ Fe^{II}Fe^{III}_2\ (SO_4)_4 \cdot 14\ H_2O \rightarrow 22\ Fe^{2+} + 30\ SO_4^{2-} + 16\ H^+ + 90\ H_2O. \qquad (6)$$

Other iron-sulfate hydrate minerals, including copiapite and coquimbite, can also provide Fe^{3+} for FeS_2 oxidation in anoxic, acidic systems. Ferric oxyhydroxides are not a likely source because they are relatively insoluble and will neutralize acid upon dissolution. For example, the overall reaction combining the oxidation of pyrite and dissolution of ferrihydrite consumes H^+ in the absence of O_2:

$$FeS_2 + 14\ Fe(OH)_3 + 26\ H^+ \rightarrow 15\ Fe^{2+} + 2\ SO_4^{2-} + 34\ H_2O. \qquad (7)$$
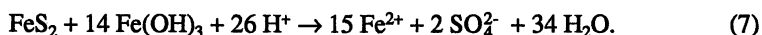
Equivalent reactions with goethite or hematite also consume H^+.

Mine Location, Geology, and Hydrology

The study area consists of a reclaimed 60-ha (hectare) surface coal mine in the bituminous field of western Pennsylvania that includes a steep-sided, broad hilltop bounded by two small tributary streams that flow northward and westward (Figure 1). Acidic seepage from the mine-spoil banks and the exposed, underlying bedrock flows into these tributaries. Land-surface altitudes at the mine range from greater than 450 m (meters) to less than 360 m above sea level (National Geodetic Vertical Datum of 1929).

Three 0.8-m-thick seams of bituminous coal were mined by use of a dragline and front-end loader to remove the overburden and coal, respectively. Because about half of the area was mined only for the lower Kittanning coal (hilltop) and the other half only for the upper and lower Clarion coals (hillside), a highwall was created that separated upper and lower benches (Figure 2). During mining, the mine was backfilled with overburden and coal-waste material. At the completion of mining in 1981, the mine spoil was regraded into a terraced configuration corresponding to the upper and lower benches. Thickness of the mine spoil averages about 15 m on the upper bench and 21 m on the lower bench. During spring 1986, a mixture of composted wood chips and municipal sewage sludge was spread at a density of about 135 T/ha (tonnes per hectare) over 24 ha of the mine-spoil surface on the lower bench. The sludge-covered area was seeded with grasses and legumes (Figure 1).

After reclamation, nests of monitor wells were installed in drill holes to evaluate the geology, hydrology, and hydrochemistry of the study area (Figure 1). In particular, two well nests were located along a line roughly parallel to the principal direction of ground-water flow (Figures 1 and 2). Nest 14 consists of 4 wells (14, 14A, 14B, 14C) in the untreated zone and nest 15 consists of 3 wells (15, 15A, 15B) in the sludge-covered zone. Each well was constructed of polyvinyl chloride (PVC) pipe in separate drill holes.
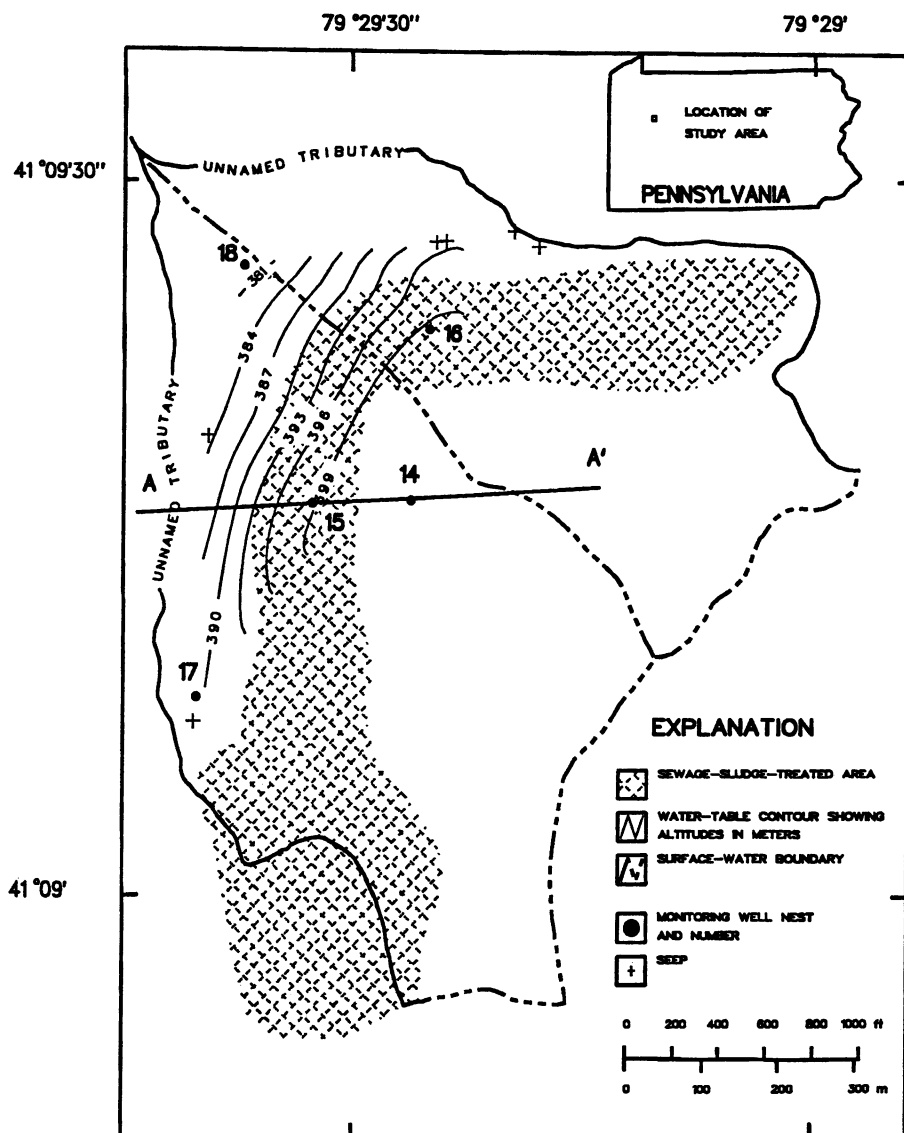
Figure 1.   Location of reclaimed surface coal mine, sewage-sludge-covered area, hydrologic monitoring sites, and configuration of water table. Line A-A' is trace of geologic section shown in Figure 2.
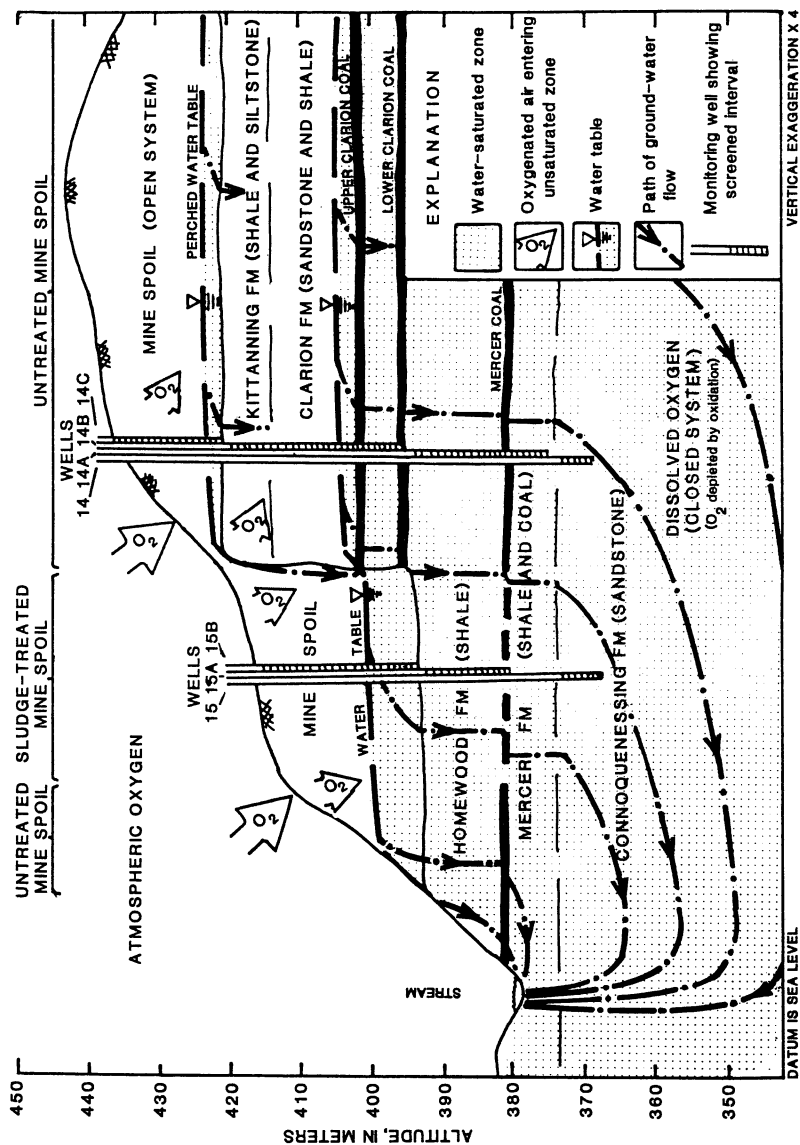
Figure 2.   East-west geologic section through the mine showing water tables and simulated flow directions reported by Saad and Cravotta (10, 25). Trace of section shown in Figure 1.

Geology. The study area is underlain by a series of sandstones, shales, and coals (Figure 2) of Pennsylvanian age that comprise (from oldest to youngest) the Connoquenessing, Mercer, and Homewood Formations of the Pottsville Group, and the Clarion and Kittanning Formations of the Allegheny Group (23, 24). Fine-grained, white-to-gray sandstone predominates in the overburden, and gray, interbedded shale and siltstone lie above and below the coals. Limestone is not present at the mine.

Pyrite, marcasite, and iron-sulfate minerals are present primarily in the coals, which contain 3-17 wt % total S and 2-20 wt % Fe, and have molar ratios of 1.2-2.1 inorganic S/Fe (10). The iron-sulfate minerals, including römerite, copiapite, coquimbite, and jarosite, are present as white and yellow efflorescences concentrated mainly in the upper and lower Clarion coals, but also are present in lesser quantities in the Mercer coals. Most FeS_2 oxidation probably occurred during mining when the water table in the highwall was lowered to a level at or below the base of the lower Clarion coal (Figure 2). The local abundance of FeS_2 and iron-sulfate minerals in the Clarion coals indicates that both spoiled and unmined, high-S coals can be sources of acid, Fe^{3+}, and SO_4^{2-}.

Ground-Water Hydrology. Ground water in the mine spoil and adjacent bedrock is recharged within the study area and flows westward and northward to streams that form the mine boundary (Figures 1 and 2). The mine spoil on the upper bench forms a perched aquifer with a saturated thickness of about 2.3 m. The spoil on the lower bench has a saturated thickness of about 5 m and is part of the water-table aquifer that includes the adjacent unmined rock in the highwall (Figures 1 and 2). Figure 2 shows simulated, steady-state ground-water-flow paths in the mine spoil and bedrock.

Ground-water-flow simulations were conducted by Saad and Cravotta (10, 25) using the steady-state option of the finite-difference computer program, MODFLOW (26). The resultant flow paths were computed and plotted using the program, MODPATH (27). The water table was simulated as a constant-flux (recharge) boundary; the eastern and western divides and base of the flow system were simulated as no-flow boundaries. Hydraulic conductivity [K, in cm/s (centimeter per second)] was estimated from rising-head slug tests (28) and was varied as follows: unconsolidated spoil and alluvium, $K = 10^{-2.6} - 10^{-2.0}$; coal and sandstone, $K = 10^{-3.4} - 10^{-3.0}$; and shale and underclay, $K = 10^{-6.0} - 10^{-5.6}$. Values of K were adjusted within these ranges until the differences between simulated and median values of measured heads were within 1 m. Figure 2 shows that simulated flow paths are dominantly horizontal in permeable units (spoil, coal, and sandstone) and downward in confining layers (shale and underclay). However, ground-water flow is upward near the stream-discharge zone at the western boundary of the modeled area.

Hydrochemical Data Collection and Evaluation

From December 1986 through September 1989, hydrochemical data were collected quarterly from the seven monitoring wells in nests 14 and 15 (Figure 2). Measurements of temperature, pH, DO, and platinum-electrode potential (Eh) of ground water were conducted at the wellhead following methods of Wood (29). Ground-water samples for analysis of cations (Fe, Mn, Al, Mg, Ca, Na, K) and silica (SiO_2) were filtered through 0.45-micrometer pore-size filters, transferred to acid-rinsed polyethylene bottles, and preserved with nitric acid. Unfiltered samples for

analysis of SO_4^{2-}, acidity, and alkalinity were stored in polyethylene bottles and preserved on ice. Concentrations of cations and SiO_2 were measured by inductively coupled plasma emission or atomic absorption spectrometry, and alkalinity (endpoint pH = 3.9) and acidity (endpoint pH = 8.3) were measured by titration following methods of Skougstad et al. (30). Concentration of SO_4^{2-} was measured by colorimetry, by use of the methylthymol blue method (30), which has an error in precision of about 10% attributed to dilution steps (Lynn Shafer, Pennsylvania Department of Environmental Resources, Bureau of Laboratories, oral commun., 1992). Charge balance errors were as large as 12.4%.

Table I reports the median and range of values of temperature, pH, Eh, and solute concentrations in the water from each well. Medians in Table I were used in the computer program WATEQ4F (31) to compute mineral saturation indices and in NEWBAL (32) to compute mass balance. Medians were used because travel times along ground-water flow paths were not precisely known; hence, the chronological relation of individual samples from different locations was difficult to establish. First, SO_4^{2-} concentrations were adjusted by 2-13% of the median values to achieve a charge balance; this adjustment attempts to correct for potential errors associated with the analytical method for SO_4^{2-} and the use of median values instead of reported data for individual water samples. After adjusting SO_4^{2-} concentrations, WATEQ4F was used to compute concentrations of the solutes, including Fe^{2+} and total CO_2, as mmol/kg. Computations of total CO_2 concentrations required alkalinity data, which were not available for waters with pH less than 3.9; thus, a concentration of C = 6.78 mmol/kg (corresponding to Pco_2, of approximately 0.1 atmosphere) was assumed. Lastly, solute concentrations were used to compute the operational redox state (RS), which is used in NEWBAL to account for electron transfer (32).

The saturation index (SI) indicates the thermodynamic potential for dissolution or precipitation of a solid phase by the ground water (3, 33-35) and provides a constraint for mass-balance models indicated by:

$$\text{Initial Solution 1 + Initial Solution 2 + Reactant Phases - Product Phases} \rightarrow \text{Final Solution.} \quad (8)$$

The initial and final solutions are the molal compositions of waters from respective upflow and downflow zones along a flow path. More than one initial solution indicates mixing of source waters. Equation 8 can be simplified to include only one initial solution. The reactant and product phases are solid or aqueous phases that can feasibly react to produce or remove elements and balance electrons. If SI is a negative number, the water is undersaturated with the solid phase and can dissolve it as a reactant. If SI is a positive number, the water is supersaturated and cannot dissolve the solid phase, but can potentially precipitate it as a product. Table II shows the computed values of SI for selected solid phases. For some minerals, such as muscovite, even though SI is positive, precipitation under surface temperature and pressures is not likely because of kinetic factors. Nevertheless, SI values for muscovite and other silicate minerals are shown in Table II to indicate potential for their dissolution. Thermodynamic data were not included in WATEQ4F for microcline, römerite, copiapite, or coquimbite, so SI values for these minerals could not be calculated. However, ground water at the mine is consistently undersaturated with respect to adularia ($KAlSi_3O_8$; SI < -1), albite ($NaAlSi_3O_8$; SI < -3), melanterite ($FeSO_4 \cdot 7H_2O$; SI < -2), and ferric sulfate ($Fe_2(SO_4)_3$; SI < -22) included in WATEQ4F.

Table I. Median and range of field measurements, major-element concentrations, and operational redox state in ground-water samples collected during 1986-89 [a]

[units are millimoles per kilogram of water, except as noted; values are median (low/high)]

Field measurements	Well number						
	Well 14	Well 14A	Well 14B	Well 14C	Well 15	Well 15A	Well 15B
Head (m)	401.5 (400.8/402.3)	401.5 (400.8/402.3)	401.5 (400.8/402.3)	423.1 (422.5/423.4)	384.4 (378.9/386.8)	392.9 (392.3/398.7)	399.0 (397.2/399.6)
Temp (°C)	12.0 (7.0/15.0)	12.0 (9.0/14.0)	12.0 (8.0/14.0)	11.0 (8.0/14.5)	11.5 (10.0/14.0)	12.0 (10.0/13.5)	12.0 (10.5/15.5)
NetAlk (g/kg)[b]	-.084 (-.244/-.020)	-.045 (-.233/-.010)	.034 (-.060/.143)	-.319 (-.469/-.299)	-1.71 (-3.60/-1.10)	-3.00 (-7.60/-.30)	-1.50 (-6.50/-.61)
pH (units)	5.80 (5.10/6.20)	5.90 (5.50/6.10)	5.92 (5.60/6.50)	3.50 (3.20/3.80)	3.12 (2.50/3.50)	2.73 (2.40/3.40)	2.75 (2.50/3.40)
Eh (volts)	.36 (.34/.41)	.33 (.28/.35)	.31 (.29/.34)	.64 (.64/.64)	.58 (.55/.60)	.59 (.53/.60)	.60 (.55/.62)
DO	.010 (.007/.023)	.011 (.007/.014)	.008 (.005/.019)	.008 (.008/.008)	.010 (.005/.012)	.008 (.004/.030)	.013 (.005/.034)
Elements[c]							
Ca	8.684 (6.986/10.479)	8.796 (7.735/9.356)	8.646 (5.988/10.479)	1.904 (1.497/2.183)	9.479 (6.986/12.974)	9.355 (7.236/10.978)	8.522 (5.739/11.477)
Mg	11.080 (9.461/15.220)	11.160 (9.872/12.135)	10.810 (7.404/11.929)	3.752 (3.332/4.114)	11.740 (10.284/13.986)	13.560 (10.695/18.100)	12.950 (9.461/15.631)
Na	.303 (.217/.413)	.263 (.226/.335)	.333 (.252/.357)	.117 (.096/.178)	.272 (.139/.370)	.184 (.117/.391)	.197 (.135/.365)
K	.223 (.197/.460)	.199 (.182/.371)	.221 (.002/.307)	.179 (.002/.207)	.177 (.128/.307)	.143 (.084/.358)	.146 (.092/.179)
C[b]	8.370	8.170	9.400	14.400	[6.780]	[6.780]	[6.780]
S (adjusted)[d]	21.630 (15.615/24.984)	21.590 (14.574/22.902)	20.760 (17.697/22.902)	8.849 (7.495/10.410)	37.953 (29.148/57.776)	49.000 (22.902/104.102)	34.930 (18.738/83.281)
Fe	1.821 (1.200/2.865)	1.776 (1.343/2.596)	1.614 (1.289/2.149)	1.762 (1.522/1.970)	9.277 (6.446/14.861)	14.030 (.788/44.763)	5.954 (.895/34.020)
Fe^{2+}[e]	1.763	1.748	1.600	1.370	9.036	13.500	5.674
Mn	.732 (.564/.946)	.735 (.637/.892)	.734 (.528/.892)	.323 (.237/.364)	1.103 (.819/1.274)	1.138 (.746/1.547)	1.123 (.619/1.456)
Si	.259 (.153/.350)	.236 (.152/.333)	.255 (.166/.516)	1.016 (.899/1.115)	.926 (.599/1.165)	1.458 (.400/1.831)	1.046 (.516/1.515)
Al	.015 (.002/.032)	.009 (.002/.041)	.009 (.002/.115)	.549 (.445/.890)	3.800 (1.705/7.413)	6.510 (1.371/20.015)	3.522 (1.186/15.567)
RS[f]	168.424	167.270	166.870	115.256	275.821	351.986	251.134

a. Quarterly data collected by USGS for 3 years during 1986-89, which resulted in a total of 12 values for most constituents to determine the median and range. DO and Eh were measured only during 1988-89, which resulted in a total of 4 data values. Only one water sample could be obtained from well 14C in 1988-89, which resulted in a total of 8 data values for most constituents and 1 value for DO and Eh.

b. NetAlk = alkalinity - acidity, in g/kg as $CaCO_3$; acidic water defined as NetAlk < 0, and alkaline water defined as NetAlk > 0. Alkalinity and acidity were titrated in the laboratory. Total CO_2, in mmol/kg as C, calculated in WATEQ4F (31) by use of alkalinity and pH; value of 6.78 mmol/kg assumed where alkalinity below detection.

c. For element concentrations in milligrams per liter, only two or three significant figures were input to WATEQ4F (31); however, concentrations in millimoles per kilogram are reported to three decimal places to avoid rounding errors in mass-balance calculations.

d. Median sulfate adjusted to attain ionic charge balance within 1%.

e. Ferrous iron computed in WATEQ4F (31) by use of measured total dissolved iron and Eh.

f. Operational redox state (RS) is treated as an element in mass-balance calculations (32, 34), where: $RS = 6 \cdot S + 4 \cdot C + 2 \cdot Fe^{2+} + 3 \cdot Fe^{3+} + 2 \cdot Mn$.

Table II. Saturation indices[a] for water samples collected during 1986-89

[values are unitless; --, insufficient data for computation]

Solid-phase name	Chemical formula	Well number						
		14	14A	14B	14C	15	15A	15B
Calcite	$CaCO_3$	-1.7	-1.5	-1.4	-6.5	--	--	--
Gypsum	$CaSO_4 \cdot 2H_2O$	-.2	-.2	-.2	-.9	-.1	-.1	-.1
Rhodochrosite	$MnCO_3$	-.8	-.6	-.6	-5.3	--	--	--
Manganite	$MnOOH$	-6.0	-6.3	-6.6	-8.2	-10.1	-11.1	-10.8
Pyrolusite	MnO_2	-11.0	-11.6	-12.2	-10.5	-13.9	-15.0	-14.5
Siderite	$FeCO_3$	-.4	-.2	-.2	-4.6	--	--	--
Ferrihydrite	$Fe(OH)_3$	2.2	2.0	1.7	.3	-1.3	-2.1	-2.2
Goethite	$FeOOH$	6.2	5.9	5.6	4.2	2.6	1.8	1.7
Melanterite	$FeSO_4 \cdot 7H_2O$	-2.9	-2.9	-2.9	-3.1	-2.1	-1.9	-2.3
Ferric sulfate	$Fe_2(SO_4)_3$	-32.7	-33.8	-34.6	-23.6	-23.2	-22.4	-23.0
Hydronium jarosite	$(H_3O)Fe_3(SO_4)_2(OH)_6$	4.1	2.9	1.9	6.9	4.4	3.6	3.1
Jarosite	$NaFe_3(SO_4)_2(OH)_6$	6.0	4.9	4.0	6.2	3.6	2.2	1.8
Natrojarosite	$KFe_3(SO_4)_2(OH)_6$	9.6	8.5	7.5	10.1	7.1	5.9	5.4
Alunite	$KAl_3(SO_4)_2(OH)_6$	5.9	5.3	5.3	-.8	-1.2	-2.9	-3.4
Alum	$KAl(SO_4)_2 \cdot 12H_2O$	-9.5	-10.0	-10.0	-7.5	-6.4	-6.3	-6.6
Al-hydroxysulfate	$AlOHSO_4$	.1	-.2	-.3	.1	.5	.3	.1
Al-hydroxysulfate	$Al_4(OH)_{10}SO_4$	6.0	5.4	5.4	-6.9	-9.0	-12.0	-12.5
Albite	$NaAlSi_3O_8$	-3.6	-3.8	-3.5	-8.8	-9.8	-10.7	-11.2
Adularia	$KAlSi_3O_8$	-1.0	-1.1	-.9	-5.9	-7.2	-8.1	-8.6
Muscovite	$KAl_3Si_3O_{10}(OH)_2$	8.4	8.0	8.3	-5.2	-8.1	-10.8	-11.5
Illite	$K_{.6}Mg_{.25}Al_{2.3}Si_{3.5}O_{10}(OH)_2$	1.2	.9	1.1	-9.4	-11.7	-13.6	-14.3
Chlorite 14Å	$Mg_5Al_2Si_3O_{10}(OH)_8$	-17.3	-16.7	-16.3	-49.2	-53.1	-57.9	-58.2
Kaolinite	$Al_2Si_2O_5(OH)_4$	3.7	3.4	3.5	-3.8	-5.5	-7.0	-7.4
Allophane (am)	$[Al(OH)_3]_{(1-x)}[SiO_2]_x$	.1	.0	.1	-1.0	-1.0	-.8	-.9
Gibbsite (c)	$Al(OH)_3$	1.1	1.0	1.0	-3.3	-4.1	-5.0	-5.1
Al-hydroxide (am)	$Al(OH)_3$	-.7	-.8	-.8	-5.0	-5.8	-6.8	-6.8
Chalcedony	SiO_2	.1	.1	.1	.7	.7	.8	.7
Silica (am,L)	$SiO_2 \cdot nH_2O$	-.4	-.5	-.4	.2	.2	.3	.2

a. Saturation index, $SI = log(IAP/K_{sp})$. Computations performed using WATEQ4F (31) with data in Table I, which consist of median chemical concentrations, temperature, pH, and Eh.

The concept of water-unsaturated, oxygenated zones (open system) versus water-saturated, O_2-limited zones (closed system) provides a basis for evaluating the location and extent of oxidation reactions in the subsurface (36). For example, DO in water at 6 °C (degrees Celsius), the minimum temperature of ground water at the site, can attain a saturation concentration of 0.38 mmol/kg (33). As this O_2-saturated water flows downward from the water table, oxidation reactions will consume the O_2. In an open system, DO will be replenished and oxidation reactions will not be limited by O_2 supply. In a closed system, however, DO will be depleted at some point along the flow path (Figure 2). Thus, if pyrite is oxidized in a closed system according to reaction 1, where 1 mol of FeS_2 reacts with 3.75 mol of O_2 to produce 2 mol of SO_4^{2-}, then reaction with 0.38 mmol/kg O_2 can produce only 0.20 mmol/kg SO_4^{2-}. Additional and potentially much greater quantities of SO_4^{2-} may be produced in the absence of DO by oxidation of FeS_2 by Fe^{3+}.

Geochemical Evolution of Acidic Ground Water

This section describes the hydrochemical trends along flow paths through the mine spoil and bedrock and evaluates the roles of O_2, pyrite, and iron-sulfate minerals in producing acidic ground water.

Hydrochemical Trends. Water from wells in nests 14 and 15, from untreated and sludge-treated zones, respectively, contains negligible concentrations of DO (< 0.034 mmol/kg) and has differing net alkalinity, pH, and Eh (Table I). Water from wells in nest 15 is more acidic, has lower pH (< 3.5) and higher Eh (> 0.5 volts), and contains greater overall solute concentrations relative to water from equivalent horizons at nest 14. At nests 15 and 14, water from the mine spoil (wells 15B and 14C) is less mineralized than the water from underlying bedrock (wells 15A and 14B), which contains elevated concentrations of SO_4^{2-} and base cations. Along flow paths, concentrations of S in ground water generally do not increase in stoichiometric proportion with Fe (S/Fe > 2) relative to pyrite (S/Fe = 2). These trends suggest, firstly, that acid produced by the oxidation of FeS_2 in the mine spoil is neutralized by reactions with silicate and carbonate minerals in the underlying bedrock. Secondly, because of neutralization along the flow path, Fe can be removed from solution by precipitation of jarosite and (or) ferrihydrite, since the water in bedrock is supersaturated with one or both of these minerals. Thirdly, intermediate concentrations of major solutes in water from well 15 relative to those farther up the flow path may result by mixing (dilution) of highly mineralized water from overlying material with less mineralized water from the east.

Supplemental data for ground-water head, pH, and sulfate concentrations during the period 1982-91, which were collected by the coal-mining company, are presented as time series in Figure 3. These data indicate the potential for transport of a previously formed plume of acidic, mineralized water from upgradient to downgradient zones and for additional oxidation reactions along the flow path(s). However, they do not indicate a simple trend of decreasing FeS_2 oxidation over time. Through 1989, pH generally was unchanged or decreased and sulfate concentration increased in the mine spoil (wells 14C and 15B) and adjacent bedrock (wells 14B, 15A, and 15), while the saturated thickness of mine spoil was relatively constant. During 1988-89, the most acidic and mineralized water was sampled from zones beneath the sludge-covered area (wells 15B and 15A). The absence of a time lag between peak sulfate concentrations in upgradient (well 15B) and downgradient (well 15A) waters and the larger sulfate concentrations in downgradient waters support the argument for sulfide oxidation along the flow path.

Inverse Modeling. Inverse modeling is used to identify and quantify the geochemical processes that cause ground-water-quality trends. Such modeling assumes that paths of ground-water flow are well defined, the stoichiometries of reactants and products are known, and the composition of the upgradient water when it began moving along the flow path is known (34, 35). For calculations herein, the composition of the upgradient water, as determined by sampling during the study, is assumed to be that of the initial water. By producing a set of models to explain changes among several locations along a flow path, the models begin to account for the sequence of reactions over distance or time. Because mass-balance models typically are not unique--many different minerals can be reacted or produced to
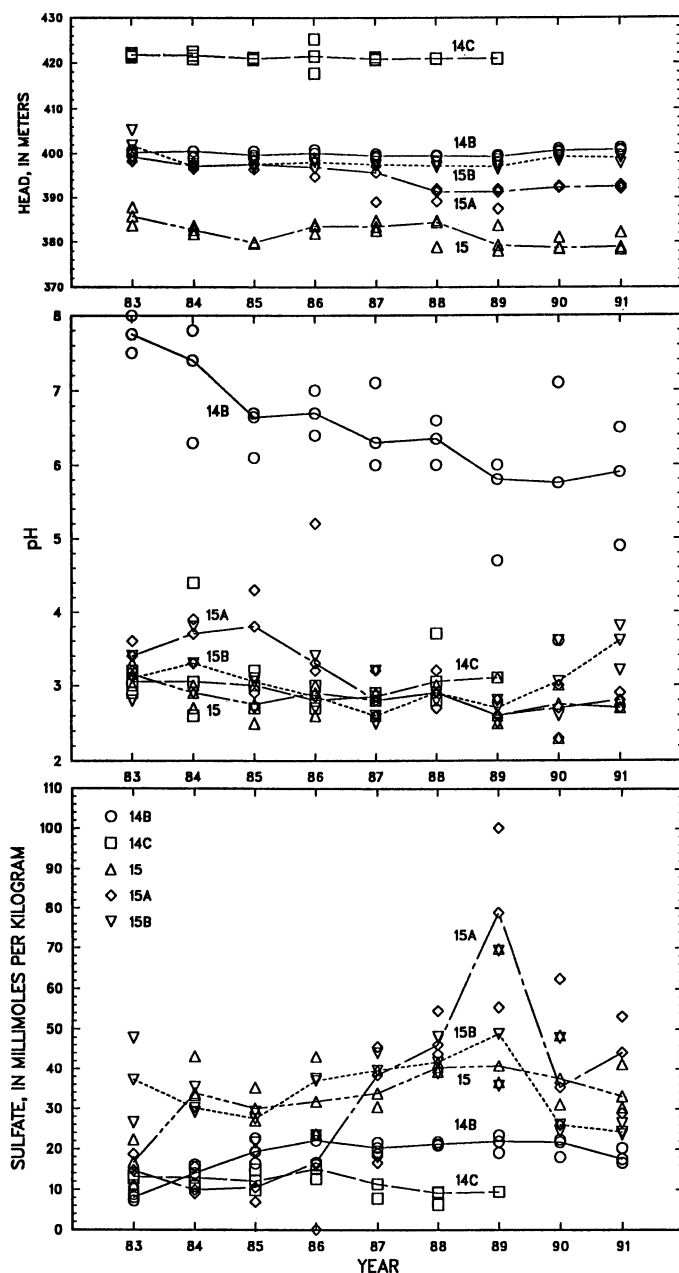
Figure 3.   Median and range of values for ground-water head, pH, and sulfate concentrations, summarized by year (e.g. "83" represents June 1982 - May 1983). For a particular sampling location, lines connect annual medians. Data were collected quarterly by the coal-mining company and are comparable with data reported in Table I, which were collected at the same locations but on different dates by USGS.

achieve the same water composition--the results are constrained by thermodynamic equilibrium criteria. Specifically, acceptable mass-balance models were constrained by considering (1) the computed SI values for solid phases (Tables II and III), to allow dissolution or precipitation of appropriately saturated phases and (2) the maximum concentration of DO (= 0.38 mmol/kg), if a closed system. Furthermore, kinetic criteria were used implicitly to constrain models to dissolve or precipitate solid phases that are "active" under the conditions. For example, under conditions of increasing pH, kinetics favor the precipitation of Fe^{3+} as amorphous $Fe(OH)_3$ or ferrihydrite, even though goethite (FeOOH) and hematite (Fe_2O_3) are less soluble (3, p. 234-237).

On the basis of simulated, steady-state flow paths in Figure 2, the following four inverse modeling scenarios were evaluated to assess the feasibility of FeS_2 oxidation in different zones, which can be open or closed with respect to O_2:

I. Open--Flow from untreated spoil (well 14C) to underlying bedrock (well 14B);

II. Open--Waters from untreated spoil (well 14C) and unmined coal (well 14B) mixed beneath sludge-treated spoil (well 15B);

III. Closed--Flow from sludge-treated spoil (well 15B) to underlying bedrock (well 15A);

IV. Closed--Waters from bedrock below untreated (well 14B) and sludge-treated (well 15A) areas mixed in deep bedrock below sludge-treated area (well 15).

Table I shows the concentrations of elements in ground water from the wells, and Table III shows the stoichiometry of potential reactant or product minerals and gases, including O_2 and CO_2. Table IV summarizes the results of the mass-balance calculations, which indicate the integrated, average quantities of reactants and products involved in reactions along the flow path(s). Minerals indicated in Table II were confirmed to be present in the mine spoil and bedrock (10), with the exception of pyrolusite, which likely is present in joints and fractures in the weathered zone. Römerite is the iron-sulfate reactant used in the models, because mixtures of ferrous and ferric sulfate hydrates are common in coal spoil (6, 11, 14), and the composition of römerite is equivalent to a 1:1 mixture of coquimbite and melanterite. In this evaluation, römerite dissolution represents the effects on the ground water from past pyrite oxidation in zones which were previously unsaturated, but which are presently below the water table and along the flow path.

I. Open system: Downward flow from untreated spoil to underlying bedrock.

Perched ground water can flow downward from untreated mine spoil (well 14C) to the underlying bedrock aquifer (well 14B). This flow path is not water-saturated, and thus is open to O_2. The water in spoil is acidic; however, the water in underlying bedrock is alkaline, has greater concentrations of S, Mn, Ca, Mg, Na, and K, and has lesser concentrations of Fe, Si, and Al (Table I). The bedrock water is supersaturated with ferrihydrite, jarosite, natrojarosite, gibbsite, chalcedony (silica phase), and kaolinite (Table II), which can precipitate and remove Fe, Na, K, Si, and Al from solution.

Table III. Stoichiometry,[a] reactivity,[b] and operational redox state[c] (RS) of potential reactant and product phases used in mass-balance computations

[units are millimoles per millimole; +, dissolution or ingassing only; -, precipitation or outgassing only]

Phase										
O_2 Gas	+RS	4.00								
Pyrite	+Fe	1.00	S	2.00	RS	.00				
Römerite	+Fe	3.00	S	4.00	RS	32.00				
Ferrihydrite	Fe	1.00	RS	3.00						
Natrojarosite	-Na	1.00	Fe	3.00	S	2.00	RS	21.00		
Jarosite	-K	1.00	Fe	3.00	S	2.00	RS	21.00		
Pyrolusite	+Mn	1.00	RS	4.00						
Siderite	+Fe	.865	Mn	.015	Mg	.02	Ca	.10	C 1.00	RS 5.76
Calcite	+Ca	1.00	C	1.00	RS	4.00				
Chlorite	+Mg	5.00	Al	2.00	Si	3.00				
Microcline	+K	.85	Na	.15	Al	1.00	Si	3.00		
Kaolinite	Al	2.00	Si	2.00						
Amorph. silica	-Si	1.00								
CO_2 Gas	-C	1.00	RS	4.00						

a. Stoichiometry excludes hydrogen and oxygen (32). Siderite stoichiometry reported by Morrison et al. (37).
b. Reactivity defined by saturation index (SI, Table II): '+' indicates reactant (SI < 0); '-' indicates product (SI > 0); no sign indicates SI could be positive or negative depending on the particular sample.
c. Redox state for minerals computed considering redox active components (S, C, Fe, Mn, O) as defined by Parkhurst et al. (32). See footnote f in Table I.

Four models were developed that satisfy mineral-solubility constraints and can be used to explain the differences in water chemistry between zones sampled by wells 14C and 14B (Table IV). The major distinction among the models is the source of 11.7 mmol/kg SO_4^{2-} as S and of 0.41 mmol/kg Mn added along the flow path. Production of S from pyrite and Mn from impure siderite (37) would require 32.6 mmol/kg of O_2 (model 1). However, if römerite and pyrolusite react (model 4), the same quantity of S can be generated with only 0.63 mmol/kg O_2. In all four models, calcite, chlorite, and microcline also are reactants; ferrihydrite, jarosite, kaolinite, amorphous silica, and CO_2 are products.

II. Open system: Waters from untreated spoil and unmined coal (highwall) mixed beneath sludge-treated spoil. Ground water can flow laterally from the intact Clarion coal horizon (well 14B) and flow vertically from the perched aquifer (well 14C) to the sludge-covered mine spoil on the lower bench (well 15B). Because the water table defines this path of ground-water mixing, the system is probably open with respect to O_2. The water of the lower bench contains greater concentrations of S, Fe, Mn, Mg, Si, and Al, intermediate concentrations of Ca and Na, and lesser concentrations of K relative to source waters upgradient along the flow paths (Table I); mixing of the source waters can produce the intermediate Ca and Na concentrations. The water of the lower bench is supersaturated with jarosite, natrojarosite, and amorphous silica (Table II), which can precipitate and remove Fe, Na, K, and Si from solution.

Table IV. Summary of mass-balance results

[All mineral and gas mass-transfers are in millimoles per kilogram of water; negative for precipitation or outgassing, positive for dissolution or ingassing; • indicates no reaction occurred. Input data are median values in Table I; mineral stoichiometry and reactivity in Table III]

Well and model no.[a]	Mixing ratio	O_2 gas	Pyrite	Römerite	Ferrihydrite	Natro-jarosite	Jarosite	Pyrolusite	Siderite	Calcite	Chlorite	Microcline	Kaolinite	Amorphous silica	CO_2 gas
I. Well 14B															
1	•	32.63	7.14	•	-27.44	•	-1.18	•	27.40	4.00	1.30	1.44	-2.29	-4.40	-36.40
2	•	26.50	7.14	•	-3.74	•	-1.18	0.41	•	6.74	1.41	1.44	-2.40	-4.51	-11.74
3	•	6.76	•	3.57	-31.01	•	-1.18	•	27.40	4.00	1.30	1.44	-2.29	-4.40	-36.40
4	•	.63	•	3.57	-7.31	•	-1.18	.41	•	6.74	1.41	1.44	-2.40	-4.51	-11.74
II. Well 15B 14B:14C															
1	98:2	31.12	8.62	•	•	.32	-1.11	.40	•	•	.45	1.22	.69	-5.62	-2.71
2	98:2	16.36	4.50	2.75	•	.52	-2.28	.40	•	•	.45	2.60	•	-8.37	-2.71
3	94:6	37.22	10.11	•	•	.50	-2.19	.41	2.62	•	.50	2.49	•	-8.20	-5.53
4	78:22	38.01	10.48	•	•	.37	-1.68	.48	•	1.39	.74	1.90	•	-7.32	-5.13
III. Well 15A															
1	•	23.19	6.64	0.21	•	-.01	-.00	•	1.00	.73	.12	•	1.38	-2.69	-1.73
2	•	16.70	4.91	1.07	•	-.01	-.00	.02	•	.83	.12	•	1.34	-2.70	-.83
3	•	•	.16	4.52	•	-.34	-1.84	•	1.00	.73	.12	2.16	.30	-7.01	-1.73
4	•	•	.25	4.18	•	-.25	-1.32	.02	•	.83	.12	1.55	.60	-5.80	-.83
IV. Well 15 15A:14B															
1	31:69	22.28	6.00	•	•	-.28	-1.52	.19	3.70	.24	•	1.77	•	-5.01	-5.75
2	34:66	14.03	4.00	•	•	-.03	-.15	.23	•	.59	•	.15	.72	-1.63	-2.33
3	34:66	•	.07	2.71	•	-.25	-1.38	.23	.23	.57	•	1.60	•	-4.54	-2.54
4	34:66	•	.09	2.61	•	-.23	-1.25	.23	•	.59	.12	1.46	.07	-4.24	-2.33

a. Model ground-water flow paths shown in Figure 2. Well number indicates "final" water: I. well 14B ← well 14C; II. well 15B ← well 14C; III. well 15A ← well 15B; and IV. well 15 ← well 15A + well 15B. Model number arbitrarily assigned to facilitate discussion of results.

Four mixing models were developed to evaluate this scenario (Table IV). Although the mixing ratios are different in each model, all indicate a larger contribution of total flow from the unmined coal in the highwall (78-98%) than from the perched aquifer. All four models involve O_2, pyrite, and pyrolusite as reactants to produce at least 14.2 mmol/kg S and 4.2 mmol/kg Fe. Chlorite and microcline also are reactants, and jarosite, natrojarosite, amorphous silica, and CO_2 are products in all four models. Models 1, 3, and 4 involve pyrite and 31 to 38 mmol/kg O_2 as reactants; and model 2 involves pyrite, römerite, and 16.4 mmol/kg O_2 as reactants. The difference between models 1 and 2 is whether römerite or kaolinite is a reactant; the difference between models 3 and 4 is whether siderite or calcite is a reactant. All four models involve large quantities of O_2.

III. Closed system: Downward flow from sludge-treated spoil to underlying bedrock. Ground water can flow downward from the water table in sludge-treated mine spoil (well 15B) to the underlying bedrock (well 15A). This flow path is water-saturated and probably closed to O_2. The bedrock water contains greater concentrations of S, Fe, Mn, Al, Ca, Mg, and Si, lesser concentrations of Na and K (Table I), and is supersaturated with jarosite, natrojarosite, and amorphous silica (Table II).

Four models were developed to evaluate this scenario (Table IV). Pyrite and römerite are reactants in all four models. Oxygen is a reactant in only models 1 and 2. The difference between models 1 and 2 and between models 3 and 4 is whether siderite or pyrolusite is a reactant. Additional reactants include calcite, chlorite, microcline, and kaolinite; products include jarosite, natrojarosite, amorphous silica, and CO_2. Only models 3 and 4 meet the closed-system criterion for acceptability (O_2 ≤ 0.38 mmol/kg). Both closed-system models involve pyrite and römerite as reactants under anoxic conditions to produce 13.9 mmol/kg S and 8 mmol/kg Fe along the flow path. Therefore, substantial quantities of SO_4^{2-} can be generated by the dissolution of previously formed ferric-sulfate salts and by the oxidation of pyrite by Fe^{3+}, even under anoxic conditions.

IV. Closed system: Waters from bedrock below untreated and sludge-treated areas mixed in deep bedrock below sludge-treated area. Ground water can flow downward and laterally from the intact Clarion coal horizon in the highwall (well 14B) and downward from the overlying shale (well 15A) to the deep sandstone bedrock beneath sludge-covered mine spoil (well 15). This path of ground-water mixing is water-saturated and closed to O_2. The resultant water contains intermediate concentrations of all the major ions, except for Ca, which is present in concentrations greater than those in the source waters (Table I). Mixing of the source waters can produce the intermediate concentrations; reactions with calcite and (or) impure siderite can produce the increased Ca concentration. The resultant water is supersaturated with jarosite, natrojarosite, and amorphous silica (Table II).

Four mixing models were developed to evaluate this scenario (Table IV). The mixing ratios indicate a larger contribution of total flow from the weathered, unmined coal in the highwall (66-69%). Pyrite and pyrolusite are reactants in all four models. Oxygen is a reactant in only models 1 and 2, and römerite is a reactant in only models 3 and 4. The difference between models 1 and 2 and between models 3 and 4 is whether siderite or kaolinite is a reactant. Calcite and microcline also are

reactants; jarosite, natrojarosite, amorphous silica, and CO_2 are products. Models 3 and 4, which involve pyrite, römerite, and pyrolusite as reactants under anoxic conditions, meet the closed-system criterion ($O_2 \leq 0.38$ mmol/kg). The argument for acid-generating reactions by ferric ions and pyrite under anoxic conditions is supported by these models. An alternative model involves the mixing of water from the deep bedrock zone beneath the unsludged area (well 14) with water from the deep shale (well 15A), which results in similar geochemical reactions to those above (Table IV). However, oxidized minerals are not likely to be abundant, and may not be present, along deep flow paths.

Discussion.   Despite negligible concentrations of DO in the ground water, concentrations of SO_4^{2-} and acidity increased with depth along flow paths from the water table in mine spoil through underlying bedrock. One interpretation is that the downgradient water quality only reflects a mineralized plume of older water that formed in the upgradient zone under unsaturated conditions, and the rate of sulfide oxidation in the upgradient zone has decreased over time as the system became water saturated. An alternative explanation, which is evaluated in this paper, is that the downgradient water quality results from hydrogeochemical mass-transfer reactions that occur along the flow path from the upgradient zone(s). In an open system, one cannot reject a mass-balance model that involves reaction with more O_2 than was measured, because it is the integrated quantity of O_2 involved in geochemical reactions that produced the solutes in the water sample. However, in a closed system, the saturation concentration of O_2 (0.38 mmol/kg or less) is the maximum quantity of O_2 available for the integrated reactions, and the measured DO is the absolute limit of O_2 available for continued reactions. Assuming that a closed system is in effect, one can reject mass-balance models that require extreme quantities of O_2 to generate the additional SO_4^{2-}. Mass-balance models indicate that either (a) extremely large quantities of O_2, as much as 100 times the O_2 solubility, can generate observed concentrations of dissolved SO_4^{2-} from FeS_2, or (b) under anoxic conditions, Fe^{3+} from iron-sulfate minerals, such as römerite, can oxidize FeS_2 along closed-system ground-water flow paths. It is likely that in the unsaturated zone and in the vicinity of the water table, which is open to O_2, oxidation of FeS_2 by O_2 accounts for most SO_4^{2-}, Fe^{2+}, and Fe^{3+} in acidic ground water. However, in the saturated zone, where the aqueous solubility of O_2 is limiting, dissolution of iron-sulfate hydrates and oxidation of FeS_2 by Fe^{3+} can explain the increase in concentration of SO_4^{2-} with increasing depth below the water table. These findings are consistent with kinetic studies ([2], [21], [22]), which show rates of pyrite oxidation by Fe^{3+} are faster than oxidation by O_2 in acidic systems, and with oxygen isotopic measurements of SO_4^{2-} by Taylor et al. ([20], [38]), which indicate 25-100% of SO_4^{2-} in AMD can result from oxidation of FeS_2 by Fe^{3+}.

The computed masses of pyrite and römerite involved in the mass-balance models (Table IV) are reasonable. The concentrations of total sulfur in a rock core collected from the location of well 14 range from <0.01 to 17.4 wt%, which is primarily in the form of iron-sulfide and iron-sulfate minerals ([10]); mass-weighted-average concentrations of total sulfur are 0.60, 0.61, and 0.57 wt% in the rock to the base of the screened intervals of wells 14B, 14A, and 14, respectively. The largest masses of pyrite and römerite involved in the mass-balance models are 10.48 mmol (672.0 mg S) and 4.52 mmol (579.6 mg S), respectively, per 1 kg water (Table IV). If the aquifer rock has a porosity of 25%, or a bulk density of 2.0 g/cm³ (grams per

cubic centimeter), and a particle density of 2.67 g/cm^3, then 1 kg of water (=approximately 1 liter) can occupy the pores in 10.7 kg of rock. Hence, pyrite as 10.48 mmol/kg water is equivalent to a sulfur concentration of 63 mg/kg rock or 0.0063 wt%, and römerite as 4.52 mmol/kg water is equivalent to a sulfur concentration of 54 mg/kg rock or 0.0054 wt%. These concentrations are only a small fraction of the average total sulfur concentrations of 0.6 wt%.

The precipitation of jarosite and natrojarosite as a potential sink for Fe^{3+}, SO_4^{2-}, Na^+, and K^+ ions is suggested because the ground water from all wells is supersaturated with respect to these minerals. This indicates that S-bearing minerals such as pyrite and römerite react at rates greater than S could precipitate. Subsurface formation of jarosite or natrojarosite has not been confirmed, however, and their supersaturation may imply kinetic barriers to precipitation. Furthermore, Na can substitute for K in jarosite solid solution (39), and the solubility of jarosite solid solutions $[(K,Na,H_3O)Fe_3(SO_4)_2(OH)_6]$, jarosite, and natrojarosite are such that relatively large concentrations of S and Fe can remain at equilibrium in water containing low concentrations of K and Na.

In previous models for the same mass-transfer scenarios, Cravotta (10) did not adjust SO_4^{2-} concentrations to correct for charge imbalances, although he noted SO_4^{2-} concentrations probably were underestimated in the elevated-concentration (> 35 mmol/kg) range. Thus models involving reactions with more than 0.38 mmol/kg O_2 in a closed system could not be ruled out because of the propagation of errors in the computed O_2. This problem has been avoided herein by adjusting SO_4^{2-} concentrations. The overall conclusions are unchanged.

Conclusions

During and after mining, pyrite oxidation forms aqueous SO_4^{2-}, Fe^{2+}, Fe^{3+}, and iron-sulfate minerals. Römerite and other iron-sulfate hydrate minerals in mine spoil and unmined coal can be a relatively important source of SO_4^{2-} and Fe^{3+}. The iron-sulfate minerals can dissolve in recharge water or in ground water, and Fe^{3+}, which is substantially more soluble than O_2 in acidic waters, can be transported to pyrite-oxidation sites below the water table where DO is absent. Subsequent coupled reduction of Fe^{3+} and oxidation of pyritic S and (or) hydrolysis of Fe^{3+} will produce acid. Negligible concentrations of DO (< 0.034 mmol/kg), high Eh (> 0.55 volt), low pH (< 3.5), and large concentrations of SO_4^{2-} and Fe^{2+} in solution are consistent with coupled reduction of Fe^{3+} and oxidation of FeS_2. Thus, aqueous SO_4^{2-} can form under anoxic conditions by dissolution of previously formed iron-sulfate minerals and by reactions between Fe^{3+} and FeS_2.

The timing and extent of formation of soluble iron-sulfate hydrate minerals in mine spoil and in unmined rock and the potential for sustained reactions between Fe^{3+} and FeS_2 are questions that have not been entirely addressed herein. Iron-sulfate minerals do not cause AMD--they are intermediate products of FeS_2 oxidation by O_2. The oxidation products can form as a transient during mining, and they can form continuously, as a result of a sustained O_2 transport to pyritic material in unsaturated mine spoil or by evaporation of AMD. Dissolution of iron-sulfate minerals can result from infiltration of recharge water or rising ground water. However, little information is available on the subsurface formation and occurrence of the sulfate salts or on the magnitude of their effect on water quality.

To prevent AMD, some researchers have suggested that pyritic materials should be submerged below a permanent water table where low O_2 solubility will limit the extent of acid-forming oxidation reactions. However, the possibility for dewatering and in situ oxidation of unmined coal during mining and oxidation of mine spoil prior to submergence of pyritic material complicates matters. An alternative surface coal-mining method involves the segregation of pyritic rock during mining and the placement of pyritic spoil high in the backfill, to be above the water table after reclamation. Placement of pyrite above the water table allows the oxidation of pyrite by humid, oxygenated air in the unsaturated zone; however, placement of pyritic rock below the water table enables leaching of oxidation products formed during mining and allows the continued oxidation of pyrite by DO and dissolved Fe^{3+} ions. Other reclamation practices to stop FeS_2 oxidation, such as the addition of O_2-consumptive barriers, alkaline additives, or bactericides to mine spoil, also are not likely to prevent AMD if previously formed oxidation products are present.

Hydrological, mineralogical, and rock-chemical data are critically important for evaluating ground-water-quality trends. At the mine studied, more densely spaced samples of ground-water and rock within the unsaturated and saturated zones would help to locate zones of active oxidation. Missing data on heat and gaseous fluxes, pyrite and ferric-sulfate mineral distribution, and recharge infiltration through unsaturated mine spoil would help to define the rate of oxidation of pyrite above the water table. In general, data could be obtained for identical locations over a period of years including the earliest stages of mining and extending several years after mine closure. These data would provide a basis for mapping the historical sequence of reactions and would enable simulation of the coupling of the physical and chemical systems to explain the evolution of acidic ground water.

Literature Cited

1. Temple, K. L.; Koehler, W. A. Engineering Experiment Station Research Bulletin 25; West Virginia University: Morgantown, WV, 1954, 35 p.
2. Singer, P. C.; Stumm, W. Science, 1970, 167, 1121-1123.
3. Stumm, W.; Morgan, J.J. Aquatic Chemistry--An Introduction Emphasizing Chemical Equilibria in Natural Waters (2nd); John Wiley & Sons, Inc.: New York, NY, 1981.
4. Kleinmann, R. L. P.; Crerar, D. A.; Pacelli, R. R. Mining Eng. 1981, 33, 300-306.
5. Nordstrom, D. K.; Jenne, E. A.; Ball, J. W. In Chemical Modeling in Aqueous Systems; Jenne, E. A., Ed.; ACS Symposium Series 93; American Chemical Society: Washington, DC, 1979, pp 51-79.
6. Nordstrom, D. K. In Acid Sulfate Weathering; Kittrick, J. A.; Fanning D. S.; Hossner L. R., Eds.; Soil Sci. Soc. of America: Madison, WI, 1982, pp 37-63.
7. Watzlaf, G. R. In Proceedings 9th Annual National Meeting American Society for Surface Mining and Reclamation; American Society for Surface Mining and Reclamation: Princeton, WV, 1992, pp 191-205.
8. Rahn, P. H. Environ. Geol. Water Sci. 1992, 19, 47-53.
9. Backes, C. A.; Pulford, I. D.; Duncan, H. J. U.S. Bur. Mines Information Circular 9183; U.S. Gov. Printing Office: Washington, DC, 1988, Vol. 1, pp 91-96.

10. Cravotta, C. A. III. In <u>Proceedings of the 1991 National Meeting of the American Society for Surface Mining and Reclamation</u>; Oaks, W. R.; Bowden, J., Eds.; American Society for Surface Mining and Reclamation: Princeton, WV, 1991, pp 43-68.

11. Dixon, J. B.; Hossner, L. R.; Senkayi, A. L.; Egashira, K. In <u>Acid Sulfate Weathering</u>; Kittrick, J. A.; Fanning D. S.; Hossner L. R., Eds.; Soil Sci. Soc. of Am.: Madison, WI, 1982, pp 169-191.

12. Karathanasis, A. D.; Evangelou, V. P.; Thompson, Y. L. <u>J. Environ. Qual.</u> 1988, <u>17</u>, 534-543.

13. Karathanasis, A. D.; Evangelou, V. P.; Thompson, Y. L. <u>J. Environ. Qual.</u> 1990, <u>19</u>, 389-395.

14. Olyphant, G. A.; Bayless, E. R.; Harper, D. <u>J. Contam. Hyd.</u> 1991, <u>7</u>, 219-236.

15. Alpers, C. N.; Maenz, C.; Nordstrom, D. K.; Erd, R. C.; Thompson, J. M. <u>GSA Abstracts with Programs</u> 1991, <u>23</u>, 382.

16. Alpers, C. N.; Nordstrom, D. K. In <u>Proceedings 2nd International Conference on the Abatement of Acidic Drainage</u>; MEND (Mine Environment Neutral Drainage): Montreal, Quebec, Canada, 1991, Vol. 2, pp 321-342.

17. Williams, J. H.; Pattison, K. L. <u>GSA Abstracts with Programs</u> 1987, <u>19</u>, 65.

18. Temple, K. L.; Delchamps, E. W. <u>App. Microbiol.</u> 1953, <u>1</u>, 255-258.

19. Garrels, R. M.; Thompson, M. E. <u>Am. J. Sci.</u> 1960, <u>258</u>, 57-67.

20. Taylor, B. E.; Wheeler, M. C.; Nordstrom, D. K. <u>Nature</u> 1984, <u>308</u>, 538-541.

21. McKibben, M. A.; Barnes, H. L. <u>Geochim. Cosmochim. Acta</u> 1986, <u>50</u>, 1509-1520.

22. Moses, C. O.; Nordstrom, D. K.; Herman, J. S.; Mills, A. L. <u>Geochim. Cosmochim. Acta</u> 1987, <u>51</u>, 1561-1571.

23. Williams, E. G. <u>J. Paleontology</u> 1960, <u>34</u>, 908-922.

24. Berg, T. M.; McInerney, M. K.; Way, J. H.; MacLachlan, D. B. <u>Pennsylvania Geol. Survey General Geology Report 75</u>; 1983.

25. Saad, D. A.; Cravotta, C. A. III. In <u>Proceedings 1991 National Meeting American Society for Surface Mining and Reclamation</u>; Oaks, W. R.; Bowden, J., Eds.; American Society for Surface Mining and Reclamation: Princeton, WV, 1991, p 545.

26. McDonald, M. G.; Harbaugh, A.W. <u>U.S. Geol. Surv. Techniques of Water-Resources Investigations 6-A1</u>; U.S. Gov. Printing Office: Washington, DC, 1988.

27. Pollack, D. W. <u>U.S. Geol. Surv. Open-File Report 89-381</u>; U.S. Gov. Printing Office: Washington, DC, 1989.

28. Bouwer, Herman. <u>Ground Water</u> 1989, <u>27</u>, 304-309.

29. Wood, W. W. <u>U.S. Geol. Surv. Techniques of Water-Resources Investigations 1-D2</u>; U.S. Gov. Printing Office: Washington, DC, 1976.

30. Skougstad, M. W.; Fishman, M. J.; Friedman, L. C.; Erdmann, D. E.; Duncan, S. S. <u>U.S. Geol. Surv. Techniques of Water-Resources Investigations 5-A1</u>; U.S. Gov. Printing Office: Washington, DC, 1979.

31. Ball, J. W.; Nordstrom, D. K.; Zachman, D. W. <u>U.S. Geol. Surv. Open-File Report 87-50</u>; U.S. Gov. Printing Office: Washington, DC, 1987.

32. Parkhurst, D. L.; Plummer, L. N.; Thorstenson, D. C. <u>U.S. Geol. Surv. Water-Resources Investigations Report 82-14</u>; U.S. Gov. Printing Office: Washington, DC, 1982.

33. Drever, J. I. The Geochemistry of Natural Waters; Prentice-Hall, Inc.: Englewood Cliffs, NJ, 1982.
34. Plummer, L. N.; Parkhurst, D.L.; Thorstenson, D.C. Geochim. Cosmochim. Acta 1983, 47, 665-686.
35. Plummer, L.N. In First Canadian/American Conference on Hydrogeology, Practical Applications of Ground Water Geochemistry; Hitchon, B.; Wallick, E.I., Eds.; National Water Well Association: Worthington, OH, 1984, pp 149-177.
36. Champ, D. R.; Gulens, R. L.; Jackson, R. E. Can. J. Earth Sci. 1979, 16, 12-23.
37. Morrison, J. L.; Atkinson, S. D.; Scheetz, B. E. In Proceedings 1990 Mining and Reclamation Conference and Exhibition; West Virginia University: Morgantown, WV, 1990, Vol. 1, pp 249-256.
38. Taylor, B.E.; Wheeler, M.C. In this volume.
39. Alpers, C. N.; Nordstrom, D. K.; Ball, J. W. Sci. Géol., Bull. 1989, 42, 281-298.